

## Mesoscopic Wave Turbulence

V. E. Zakharov<sup>1,2,3</sup>, A. O. Korotkevich<sup>1</sup>, A. N. Pushkarev<sup>1,3</sup>, and A. I. Dyachenko<sup>1</sup>

<sup>1</sup> Landau Institute for Theoretical Physics, Russian Academy of Sciences, Moscow, 119334 Russia

<sup>2</sup> Department of Mathematics, University of Arizona, Tucson, AZ 85721, USA

<sup>3</sup> Waves and Solitons LLC, Gilbert, AZ 85233, USA

e-mail: kao@landau.ac.ru

Received August 17, 2005

We report results of simulation of wave turbulence. Both inverse and direct cascades are observed. The definition of “mesoscopic turbulence” is given. This is a regime when the number of modes in a system involved in turbulence is high enough to qualitatively simulate most of the processes but significantly smaller than the threshold, which gives us quantitative agreement with the statistical description, such as the kinetic equation. Such a regime takes place in numerical simulation, in essentially finite systems, etc. © 2005 Pleiades Publishing, Inc.

PACS numbers: 02.60.Cb, 47.11.+j, 47.27.Eq, 47.35.+i

The theory of wave turbulence is developed for infinitely large systems. In weakly nonlinear dispersive media, the turbulence is described by a kinetic equation for squared wave amplitudes (weak turbulence). However, all real systems are finite. Computer simulation of wave turbulence can also be performed only in finite systems (typically, in a box with periodic boundary conditions). It is important to know how strong discreteness of a system impacts the physical picture of wave turbulence.

Let a turbulence be realized in a  $Q$ -dimensional cube with side  $L$ . Then, wave vectors form a cubic lattice with the lattice constant  $\Delta k = 2\pi/L$ . Suppose that four-wave resonant conditions are dominating. Exact resonances satisfy the equations

$$\mathbf{k} + \mathbf{k}_1 - \mathbf{k}_2 - \mathbf{k}_3 = 0, \quad (1)$$

$$\Delta = \omega(k) + \omega(k_1) - \omega(k_2) - \omega(k_3) = 0. \quad (2)$$

In an infinite medium, Eqs. (1) and (2) define hypersurface dimension  $3Q - 1$  in  $4Q$ -dimensional space  $\mathbf{k}, \mathbf{k}_1, \mathbf{k}_2, \mathbf{k}_3$ . In a finite system, (1) and (2) are Diophantine equations, which might have or have no exact solutions. The Diophantine equations for four-wave resonant processes are not studied yet. For three-wave resonant processes, they are studied for Rossby waves on the  $\beta$  plane [1].

However, not only exact resonances are important. Individual harmonics in the wave ensemble fluctuate with inverse time  $\Gamma_{\mathbf{k}}$ , dependent on their wavenumbers. Suppose that all  $\Gamma_{\mathbf{k}_i}$  for waves composing a resonant quartet are of the same order of magnitude  $\Gamma_{\mathbf{k}_i} \sim \Gamma$ . Then, resonant equation (2) has to be satisfied up to

accuracy  $\Delta \sim \Gamma$ , and the resonant surface is blurred into the layer of thickness  $\delta k/k \approx \Gamma_{\mathbf{k}}/\omega_{\mathbf{k}}$ . This thickness should be compared with the lattice constant  $\Delta k$ . Three different cases are possible:

(1)  $\delta k \gg \Delta k$ . In this case, the resonant layer is thick enough to hold many approximate resonant quartets on a unit of resonant surface square. These resonances are dense, and the theory is close to the classical weak turbulent theory in infinite media. The weak turbulent theory offers recipes for calculation of  $\Gamma_{\mathbf{k}}$ . The weak-turbulent  $\Gamma_{\mathbf{k}}$  are the smallest among all the given by theoretical models. To be sure that the case is realized, one has to use weak-turbulent formulas for  $\Gamma_{\mathbf{k}}$ .

(2)  $\delta k < \Delta k$ . This is the opposite case. Resonances are rarefied, and the system consists of a discrete set of weakly interacting oscillators. A typical regime in this situation is the “frozen turbulence” [2–4], which is actually a system of KAM tori accomplished with a weak Arnold’s diffusion.

(3) The intermediate case  $\delta k \approx \Delta k$  can be called “mesoscopic turbulence.” The density of approximate resonances is high enough to provide the energy transport along the spectrum but low enough to guarantee “equal rights” for all the harmonics, which is a necessary condition for the applicability of the weak turbulent theory.

In this article, we report results of our numerical experiments on modeling of turbulence of gravity waves on the surface of deep ideal incompressible fluid. The motivation for this work was numerical justification of the Hasselmann kinetic equation. The result is discovery of the mesoscopic turbulence. The fluid motion is potential and described by the shape of surface  $\eta(\mathbf{r}, t)$  and the velocity potential  $\psi(\mathbf{r}, t)$  evaluated

<sup>†</sup>The text was submitted by the authors in English.

on the surface. These variables satisfy the canonical equations [5]

$$\frac{\partial \eta}{\partial t} = \frac{\delta H}{\delta \psi}, \quad \frac{\partial \psi}{\partial t} = -\frac{\delta H}{\delta \eta}, \quad (3)$$

Hamiltonian  $H$  is represented by the first three terms in expansion of powers of nonlinearity  $\nabla \eta$ :

$$\begin{aligned} H &= H_0 + H_1 + H_2 + \dots, \\ H_0 &= \frac{1}{2} \int (g\eta^2 + \psi \hat{k} \psi) dx dy, \\ H_1 &= \frac{1}{2} \int \eta [|\nabla \psi|^2 - (\hat{k} \psi)^2] dx dy, \\ H_2 &= \frac{1}{2} \int \eta (\hat{k} \psi) [\hat{k}(\eta(\hat{k} \psi)) + \eta \nabla^2 \psi] dx dy. \end{aligned} \quad (4)$$

Thereafter, we put the gravity acceleration equal to  $g = 1$ . Here,  $\hat{k}$  is a linear integral operator ( $\hat{k} = \sqrt{-\nabla^2}$ ),

such that, in  $k$  space, it corresponds to multiplication of Fourier harmonics

( $\psi_{\mathbf{k}} = \frac{1}{2\pi} \int \psi_r e^{i\mathbf{k}\mathbf{r}} dx dy$ ) by

$\sqrt{k_x^2 + k_y^2}$ . For gravity waves, this reduced Hamiltonian describes four-wave interaction. Then, dynamical equations (3) acquire the form

$$\begin{aligned} \dot{\eta} &= \hat{k} \psi - (\nabla(\eta \nabla \psi)) - \hat{k}[\eta \hat{k} \psi] \\ &+ \hat{k}(\eta \hat{k}[\eta \hat{k} \psi]) + \frac{1}{2} \nabla^2[\eta^2 \hat{k} \psi] + \frac{1}{2} \hat{k}[\eta^2 \nabla^2 \psi], \end{aligned} \quad (5)$$

$$\begin{aligned} \dot{\psi} &= -g\eta - \frac{1}{2} [(\nabla \psi)^2 - (\hat{k} \psi)^2] \\ &- [\hat{k} \psi] \hat{k}[\eta \hat{k} \psi] - [\eta \hat{k} \psi] \nabla^2 \psi. \end{aligned}$$

Let us introduce the canonical variables  $a_{\mathbf{k}}$  as shown below:

$$a_{\mathbf{k}} = \sqrt{\frac{\omega_{\mathbf{k}}}{2k}} \eta_{\mathbf{k}} + i \sqrt{\frac{k}{2\omega_{\mathbf{k}}}} \psi_{\mathbf{k}}, \quad (6)$$

where  $\omega_{\mathbf{k}} = \sqrt{gk}$ . In these so-called normal variables, equations (3) take the form

$$\frac{\partial a_{\mathbf{k}}}{\partial t} = -i \frac{\delta H}{\delta a_{\mathbf{k}}^*}. \quad (7)$$

The physical meaning of these variables is quite clear:  $|a_{\mathbf{k}}|^2$  is an action spectral density, or  $|a_{\mathbf{k}}|^2 \Delta k^2$  is a number of particles with the particular wavenumber  $\mathbf{k}$ .

We solved equations (5) numerically in a box  $2\pi \times 2\pi$  using a spectral code on a rectangular grid with double periodic boundary conditions. The implicit energy-preserving scheme is similar to that used in [6–8] was implemented. We studied the evolution of freely propagating waves (swell) in the absence of wind in the spirit of paper [9]. Different grids ( $512 \times 512$ ,  $256 \times 1024$ ,

$256 \times 2048$ ) with different initial data were tried. In all the cases, we observed mesoscopic wave turbulence. The most spectacular results are achieved on the grid  $256 \times 2048$ .

As initial conditions, we used a Gauss-shaped distribution on a long axis of the wavenumbers plane

$$\begin{cases} |a_{\mathbf{k}}| = A_i \exp\left(-\frac{1}{2} \frac{|\mathbf{k} - \mathbf{k}_0|^2}{D_i^2}\right), & |\mathbf{k} - \mathbf{k}_0| \leq 2D_i, \\ |a_{\mathbf{k}}| = 10^{-6}, & |\mathbf{k} - \mathbf{k}_0| > 2D_i, \end{cases} \quad (8)$$

$$A_i = 5 \times 10^{-6}, \quad D_i = 30, \quad \mathbf{k}_0 = (0; 150).$$

The initial phases of all the harmonics were random. The average steepness is  $\mu = \langle |\nabla \eta| \rangle \approx 0.115$ . To stabilize the computations in the high-frequency region [10], we introduced artificial damping, mimicking viscosity at small scales, and an artificial smoothing term to the equation for the surface evolution

$$\begin{aligned} \frac{\partial \psi_{\mathbf{k}}}{\partial t} &\rightarrow \frac{\partial \psi_{\mathbf{k}}}{\partial t} + \gamma_k \psi_{\mathbf{k}}, \\ \frac{\partial \eta_{\mathbf{k}}}{\partial t} &\rightarrow \frac{\partial \eta_{\mathbf{k}}}{\partial t} + \gamma_k \eta_{\mathbf{k}}, \end{aligned} \quad (9)$$

$$\gamma_k = \begin{cases} 0, & k < k_d, \\ -\gamma(k - k_d)^2, & k \geq k_d, \end{cases}$$

$$k_d = 512, \quad \gamma = 2 \times 10^4, \quad \tau = 3.1 \times 10^{-4}.$$

With the time step  $\tau$ , these calculations took about two months on an AMD Athlon 64 3500+ computer. During this time, we reached 1500 periods of the wave in the initial spectral maximum.

The process of waves evolution can be separated in two steps. On the first stage (about fifty initial wave periods), we observe fast loss of energy and wave action. This effect can be explained by formation of “slave” harmonics taking their part of motion constants. Initially, the smooth spectrum becomes very rough. The spectral maximum demonstrates a fast downshift.

In the second stage, the downshift continues but all the processes slow down. Plots of the energy, wave action, mean frequency, and mean steepness are presented in Figs. 1–4.

One can see a clear tendency to downshift of the spectral maximum corresponding to inverse cascade; however, this process is more slow than predicted by weak turbulence theory. The self-similar downshift in this theory gives [11, 12]

$$\omega \sim t^{-1/11}.$$

In our experiments,

$$\omega \sim t^{-\alpha},$$

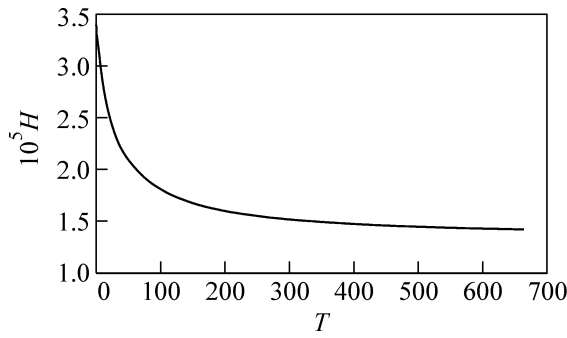


**Fig. 1.** Total energy of the system.

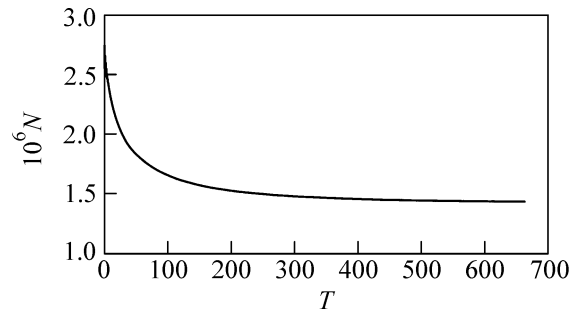


**Fig. 2.** Total action of the system.

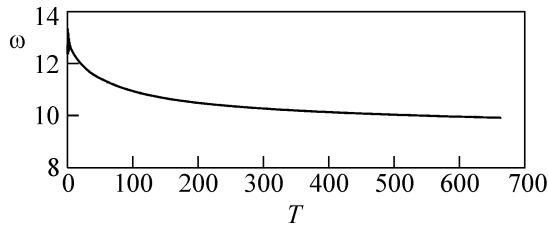


**Fig. 3.** Frequency of the spectral maximum.

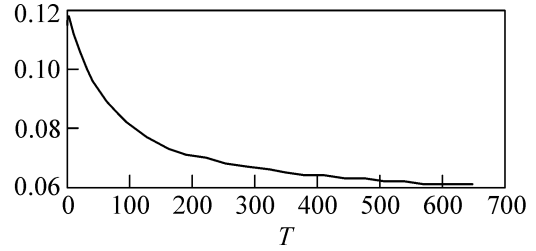


**Fig. 4.** Mean steepness of fluid surface.

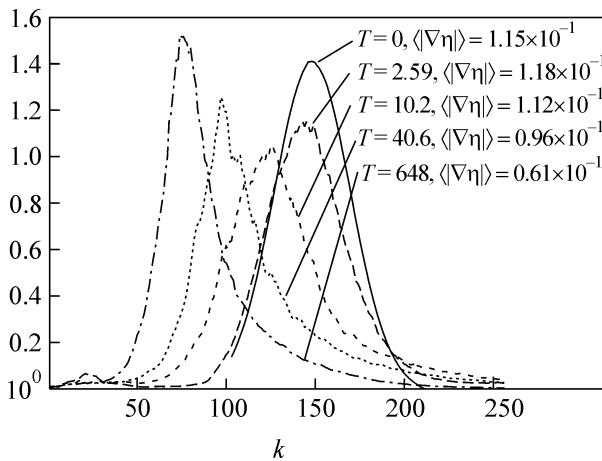


**Fig. 5.** Averaged with angle spectra. Downshift of spectral maximum is clearly observable.

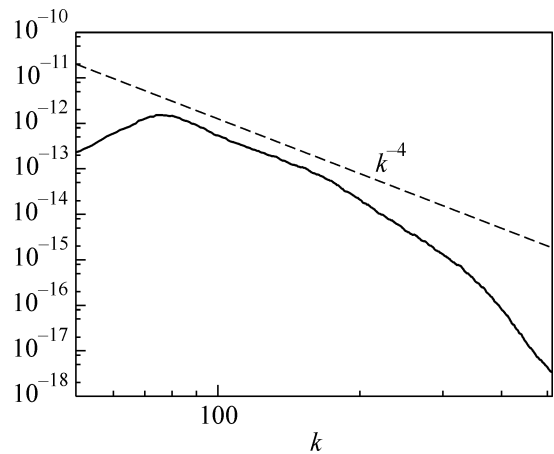


**Fig. 6.** Tails of angle-averaged spectrum in double logarithmic scale.  $T = 648 = 1263T_0$ . Powerlike tail and front slope are close to predicted by weak turbulent theory.

where  $\alpha$  decreases with time from  $1/16$  to  $1/20$ . Evolution of angle-averaged spectra  $N_k = \int_0^{2\pi} |a_{\mathbf{k}}|^2 k dk d\vartheta$  is presented in Fig. 5. Their tails (Fig. 6) are Zakharov–Filonenko weak-turbulent Kolmogorov spectra [13] corresponding to direct cascade

$$\langle |a_{\mathbf{k}}|^2 \rangle \sim 1/k^4. \quad (10)$$

This result is robust; it was observed in similar calculations [7–9].

Two-dimensional spectra in the initial and in the last moments of the calculations are presented in Fig. 7. One can see formation of small-intensity “jets” posed on the Phillips resonant curve [14]

$$2\omega(\mathbf{k}_0) = \omega(\mathbf{k}_0 + \mathbf{k}) + \omega(\mathbf{k}_0 - \mathbf{k}). \quad (11)$$

The spectra are very rough and sharp. The slice of spectra along the line  $(0; k_y)$  at the end of the computations is presented in Fig. 8. Evolution of squared wave

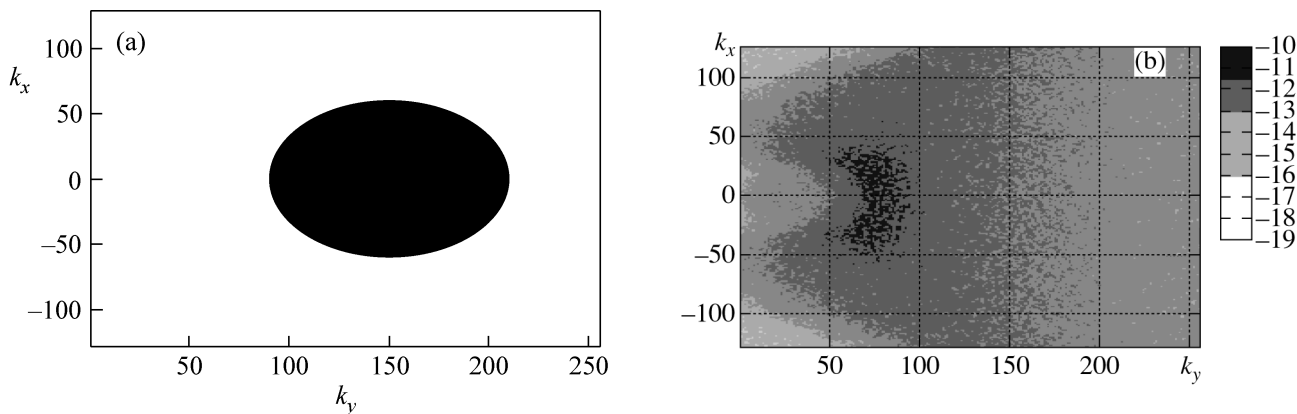


**Fig. 7.** (a) Level lines of logarithm of initial spectra distribution.  $T = 0$ . (b) Level lines of logarithm of spectra distribution at  $T = 648 = 1263T_0$ .

amplitudes for a cluster of neighboring harmonics is presented in Fig. 9.

Results presented in Fig. 9 show that what we modeled is mesoscopic turbulence. Indeed, the characteristic time of the amplitude evolution in the figure is a hundred or more of their periods; thus,  $\Gamma/\omega_k$  is comparable with  $\Delta k/k$ . In the same figure, we can see the most remarkable features of such turbulence.

The weak turbulence in the first approximation obeys the Gaussian statistics. The neighboring harmonics are uncorrelated and statistically independent ( $\langle a_k a_{k+1}^* \rangle = 0$ ). However, their averaged characteristics are close to each other. This is a “democratic society.” On the contrary, mesoscopic turbulence is an “oligarchic society.” The Phillips curve (11) has a genus of 2. After Faltings’ proof [15] of Mordell’s hypothesis [16],

we know that the number of solutions of the Diophantine equation

$$\Delta = 2(n^2 + m^2)^{1/4} - [(n+x)^2 + (m+y)^2]^{1/4} - [(n-x)^2 + (m-y)^2]^{1/4} = 0 \tag{12}$$

is at most finite and most probably, except for a few trivial solutions, equals zero. The same statement is very plausible for more general resonances. Approximate integer solutions in the case

$$|\Delta| < \epsilon$$

do exist, but their number fast tends to zero at  $\epsilon \rightarrow 0$ . Classification of these solutions is a hard problem of number theory. These solutions compose the “elite society” of the harmonics, which play the most active role in the mesoscopic turbulence. Almost all the inverse cascade of wave action is realized within mem-

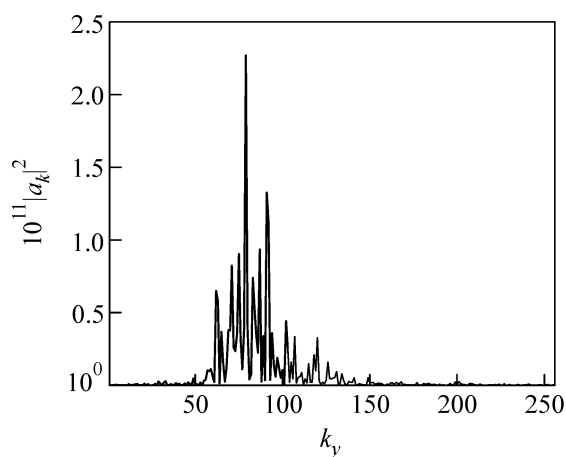


**Fig. 8.** Slice of spectrum on axis  $(0; k_y)$  at  $T = 648 = 1263T_0$ .

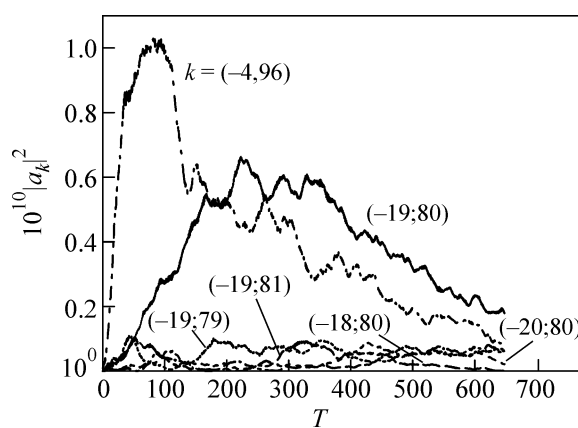


**Fig. 9.** Evolution of some cluster of harmonics and a distant large harmonic.

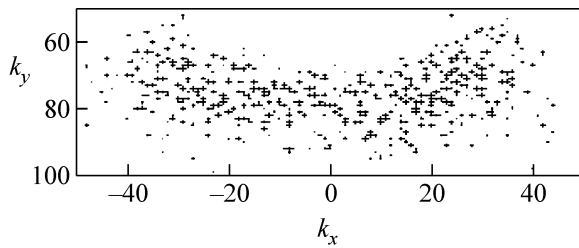


**Fig. 10.** Harmonics with square modulus exceeding level  $10^{-11}$  at  $T = 648 = 1263T_0$ .

bers of this “privileged club.” The distribution of the harmonics exceeding the reference level  $|a_k|^2 = 10^{-11}$  at the moment  $t = 1200T_0$  is presented in Fig. 10. The number of such harmonics is not more than 600, while the total number of harmonics involved into the turbulence is of the order of  $10^4$ .

Note that a situation with direct cascade is different. As far as the coupling coefficient for gravity waves grow as fast as  $k^3$  with the wave number, for short waves,  $\Gamma_k/\omega_k$  easily exceeds  $\Delta k/k$ , and the conditions of the applicability of the weak turbulent theory for short waves are satisfied.

Note also that the mesoscopic turbulence is not a numerical artifact. Simple estimations show that, for gravity waves, it is realized in some conditions in basins of a moderate size, like small lakes as well as in experimental wave tanks. It is also common for long internal waves in the ocean and for inertial gravity waves in the atmosphere, for plasma waves in tokamaks, etc.

This work was supported by the Russian Foundation for Basic Research (grant no. 03-01-00289), the program “Nonlinear Dynamics and Solitons” of the Presidium of the Russian Academy of Sciences, the “Leading Scientific Schools of Russia” grant, the ONR (grant no. N00014-03-1-0648), the US Army Corps of Engineers, the RDT & E Program no. W912HZ-04-P-0172, and by the DACA (grant no. 42-00-C0044). We use this opportunity to gratefully acknowledge the support of these foundations.

Also, the authors want to thank the creators of the open-source fast Fourier transform library FFTW [17] for this fast, portable, and completely free piece of software.

## REFERENCES

1. G. Reznik, L. Piterbarg, and E. Kartashova, *Dyn. Atmos. Oceans* **18**, 235 (1993).
2. A. N. Pushkarev and V. E. Zakharov, *Physica D (Amsterdam)* **155**, 98 (1999).
3. A. N. Pushkarev, *Eur. J. Mech. B/Fluids* **18**, 345 (1999).
4. C. Connaughton, S. Nazarenko, and A. Pushkarev, *Phys. Rev. E* **63**, 046306 (2001).
5. V. E. Zakharov, *J. Appl. Mech. Tech. Phys.* **2**, 190 (1968).
6. A. I. Dyachenko, A. O. Korotkevich, and V. E. Zakharov, *Pis'ma Zh. Éksp. Teor. Fiz.* **77**, 572 (2003) [*JETP Lett.* **77**, 477 (2003)]; physics/0308100.
7. A. I. Dyachenko, A. O. Korotkevich, and V. E. Zakharov, *Pis'ma Zh. Éksp. Teor. Fiz.* **77**, 649 (2003) [*JETP Lett.* **77**, 546 (2003)]; physics/0308101.
8. A. I. Dyachenko, A. O. Korotkevich, and V. E. Zakharov, *Phys. Rev. Lett.* **92**, 134501 (2004); physics/0308099.
9. M. Onorato, A. R. Osborne, M. Serio, *et al.*, *Phys. Rev. Lett.* **89**, 144501 (2002); nlin.CD/0201017.
10. P. M. Lushnikov and V. E. Zakharov, *Physica D (Amsterdam)* **203**, 9 (2005); nlin.PS/0410054.
11. V. E. Zakharov, PhD Thesis (Budker Inst. for Nuclear Physics, Novosibirsk, USSR, 1966).
12. V. E. Zakharov and M. M. Zaslavskii, *Izv. Akad. Nauk SSSR, Fiz. Atmos. Okeana* **18**, 747 (1982).
13. V. E. Zakharov and N. N. Filonenko, *J. Appl. Mech. Tech. Phys.* **4**, 506 (1967).
14. O. M. Phillips, *J. Fluid Mech.* **107**, 465 (1981).
15. G. Faltings, *Invent. Math.* **73**, 349 (1983); *Invent. Math.* **75**, 381(E) (1984).
16. L. J. Mordell, *Proc. Cambridge Philos. Soc.* **21**, 179 (1922).
17. M. Frigo and S. G. Johnson, in *Proceedings of 23rd International Conference on Acoustics, Speech, and Signal Processing, ICASSP-1998* (1998), Vol. 3, p. 1381; <http://fftw.org>.

SPELL: OK